Numerical simulation of two-phase combustion in a scramjet

Florian Kissel, Guillaume Ribert, Pascale Domingo
CORIA - CNRS, Normandie Université, INSA Rouen Normandie, Rouen, 76000, France

1 Introduction

In the past decades, scramjet engines have been investigated [1] to be an alternative for hypersonic flight propulsion systems because of their high specific impulse and low launch cost. Fuel ignition is a challenging issue for such engines because of the high speed of the incoming flow and the reduced length of the combustor. Within a residence time of milliseconds, it becomes difficult to obtain fuel mixing, ignition and reliable flame stabilisation [1]. Cavity flame holders have been a promising solution to enhance mixing by trapping the fuel and air in recirculation zones [2]. However, the properties of the fuel also have a significant importance in combustion mechanisms. Indeed, while the first scramjet studies were conducted by injecting hydrogen or gaseous ethylene, liquid hydrocarbon fuels are of more practical interest to use up to Mach 8 thanks to their high densities and ease of handling [3]. Over the last two decades, experimental setups were developed to study the characteristics of fuel ignition with and without pilot injection [4], fuel mixing [5], and conditions of flame blowout [5], with the conclusion that using liquid fuel requires an advanced understanding of the interactions between supersonic flow, turbulence, combustion and liquid vaporisation. Therefore, computational fluid dynamics has been frequently applied to understand the internal flow characteristics of supersonic combustion. For example, in [6,7], using liquid fuel enhances mixing between fuel and air and slows down chemistry due to the endothermic effects associated with evaporation. In addition, using more detailed combustion mechanisms allows for the reproducing of some chemical phenomena, such as the endothermic pyrolysis of kerosene into small hydrocarbon [7, 8]. In the present study, Large-Eddy Simulations (LES) are performed to reproduce the processes arising in the CARDC (Chinese Academy Research and Development Centre) combustor [9]. The main focus of this study is on the stabilisation mechanisms of the kerosene flame, the latter being injected as a spray in the scramjet's cavity.

2 Experimental and numerical configuration

The studied experimental configuration is a supersonic cavity flame holder [9]. The cavity is located 115 mm downstream of the end of the isolator and has a depth of $D = 8$ mm with a length of 45 mm. The stagnation pressure and temperature are 1.35 MPa and 1720 K, respectively. A pilot gaseous hydrogen flame is located upstream of the cavity with an equivalence ratio of 0.086. The kerosene equivalence ratio is 0.43. The geometry of the configuration, as well as boundary conditions and length for the numerical configuration, are defined in Fig. 1. The simulations have been performed with the CORIA in-house code SiTCom-B [10–14] that uses cartesian meshes. The gaseous phase is described by

Correspondence to: guillaume.ribert@insa-rouen.fr

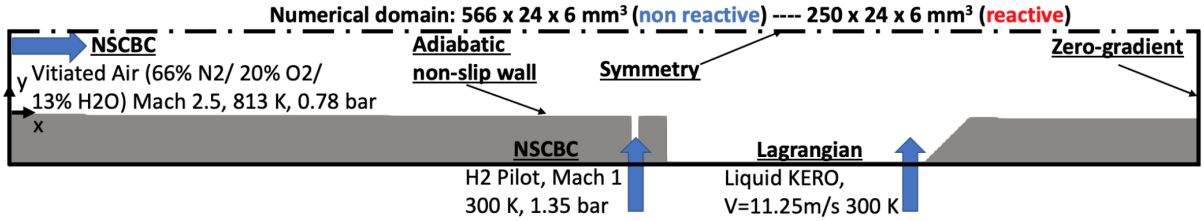

Figure 1: Sketch of the numerical configuration.

Navier-Stokes equations coupled to energy and species transport. The detailed chemistry [14] is a reduced and optimised version of the chemical mechanism of [15] that contains 18 reactive species and 29 elementary reactions. The partially stirred reactor (PaSR) approach [16] is employed to estimate the filtered species source terms. The subgrid-scale stress tensor, which is modelled in LES, is resolved with the WALE model [17]. Navier-Stokes characteristic boundary conditions (NSCBC) are applied to describe all the inlet boundary conditions, while the outflow uses a zero-gradient condition. An immersed boundary method (IBM) models the solid surface.

The main assumption concerning the liquid phase modelling is that the spray will be considered in a diluted regime meaning that the interaction between each droplet could be neglected. Since the collision and coalescence processes among droplets are neglected, the motion of an evaporating droplet in a dilute flow is simulated using the Basset-Boussinesq-Oseen (BBO) equations [18] in which the gravity, Coriolis force, centrifugal force, Basset force, and virtual mass effect are all neglected. Each drop will, therefore, be considered as a source point, while the Lagrangian-Eulerian coupling will be done using a two-way coupling. The model proposed by Henderson [19] is used for calculating the drag coefficient required in the BBO equations. The evaporation process of droplets is modelled via Abramzon-Sirignano theory [20].

3 Results

To begin with, the simulation is performed with the sole pilot flame of H_2, leading to filling the cavity with hot burnt gases. Then, the kerosene injection is added, and finally, after a few convective times, the pilot flame is stopped, leaving only the kerosene to burn. Such a scenario mimics the procedure described in [9].

The resulting flame and the structure of the spray in the cavity are shown in Fig. 2, where the temperature field is superposed to the droplet spray coloured either by the droplet residence time before total evaporation or by the droplet velocity. Most of the drops move in the opposite direction to the flow entering the cavity, and only a small amount of drops manage to cross the mixing layer above the cavity to enter the main flow. The drops are distributed along the entire depth of the cavity. The study of the residence time of the drops shows that they evaporate quasi-entirely in the cavity, where the gas temperature is relatively hot of the order of 1000 to 1500 K, with a residence time below 300 µs. The drops do not interact directly with the flame, but their evaporation, coupled with the pyrolysis of the kerosene, locally cools the mixing layer located above the injection. Since the transverse injection of kerosene is located near the main recirculation zone of the cavity, the drops follow the flow dynamics within the cavity but also modify the resulting mixing layer and recirculation zones. Indeed, as shown with the flow streamlines in Fig. 3, the recirculation in the cavity splits into two vortices, labelled 1 and 2, with the same direction of rotation, located on either side of the kerosene injection. The drops injected at the floor of the cavity are mostly deflected into the recirculation 1. Only a small proportion of the drops are entrained into recirculation 2, which is, therefore, mostly filled with burnt gases. A "dead zone" is observed at the lower corner of the leading edge of the cavity, where the speed is almost zero.

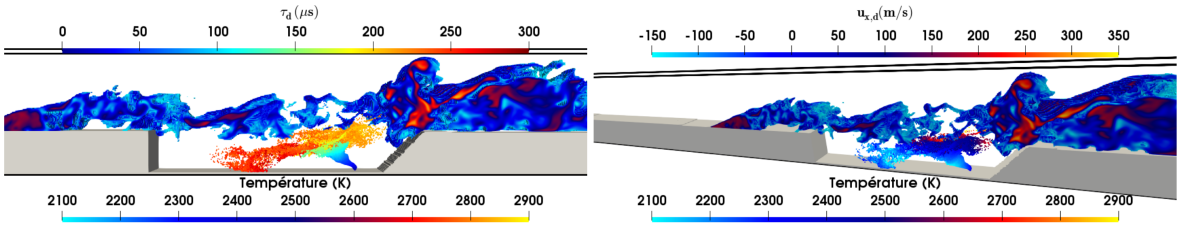

(a) (b)

Figure 2: Instantaneous field of the droplet spray with temperature field greater than 2100 K. (a): Droplets coloured by their residence times before total evaporation - (b): Droplets coloured by their velocities.

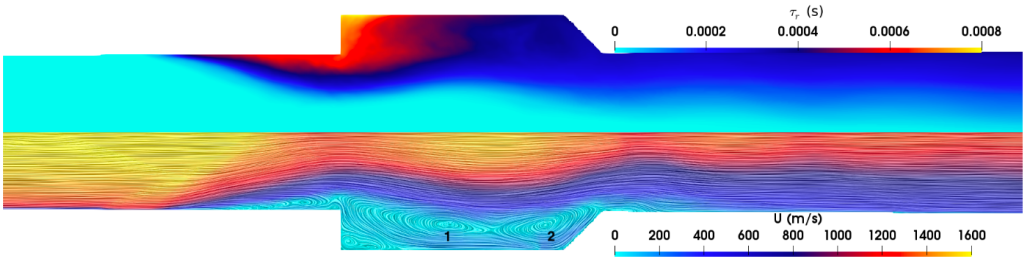

Figure 3: Average velocity field with streamlines in the combustion chamber (bottom) and gaseous kerosene residence time in the cavity (top).

Upstream of the cavity, due to the increase of the heat of combustion and an adverse pressure gradient, the separation of the boundary layer is observed, which causes a compression of the flow, characterised by an oblique shock wave and a decrease in the speed of the main flow. The sudden opening caused by the cavity creates a relaxation, which deflects the current lines towards the floor of the cavity with a characteristic wavelet shape.
Fig. 4 shows the mean field of the mixture fraction calculated according to the formulation of Bilger et al. [21], in the central plane at injection. The stoichiometric mixture fraction is equal to 0.067. The

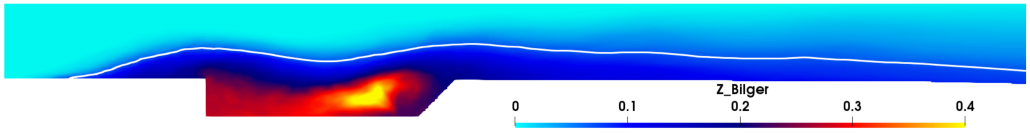

Figure 4: Mean field of the mixture fraction Z. White line: stoichiometry line $Z_{\text{st}} = 0.067$.

cavity is, therefore, very rich. Stoichiometry is reached upstream of the cavity, at the boundary layer separation, in the mixture layer and then above the downstream wall of the cavity. A large part of the fuel leaves the cavity and mixes with the oxygen located in the main flow, at the level of the mixture layer and a large part continues to burn in the divergent since the cavity does not contain oxygen. By looking at the mean field of the mass fraction of N-decane (see Fig. 5), the concentration is maximum in the cavity, around the evaporation of the spray. The fuel mixes in the cavity, following the recirculations and is completely pyrolyzed outside the cavity. The area where N-decane remains present coincides with the low-temperature zone in the cavity, due to spray evaporation. Hydrocarbons from pyrolysis react upstream of the cavity and at the ramp, where temperatures are higher, around 2200 K to 2400 K. The flow in the mixing layer above the cavity cools to a temperature of around 2000 K due to interaction

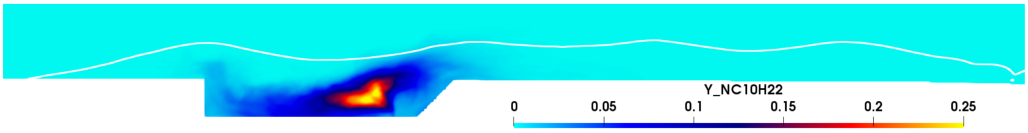

Figure 5: Mean field of the mass fraction of kerosene. White line: iso-Mach $= 1$.

with the evaporating spray and the pyrolyzing kerosene.

Fig. 6 shows the average fields of pressure, temperature and mass fractions of CO, CO_2, which are markers of incomplete or complete combustion, and O_2. The pressure upstream and in the cavity is

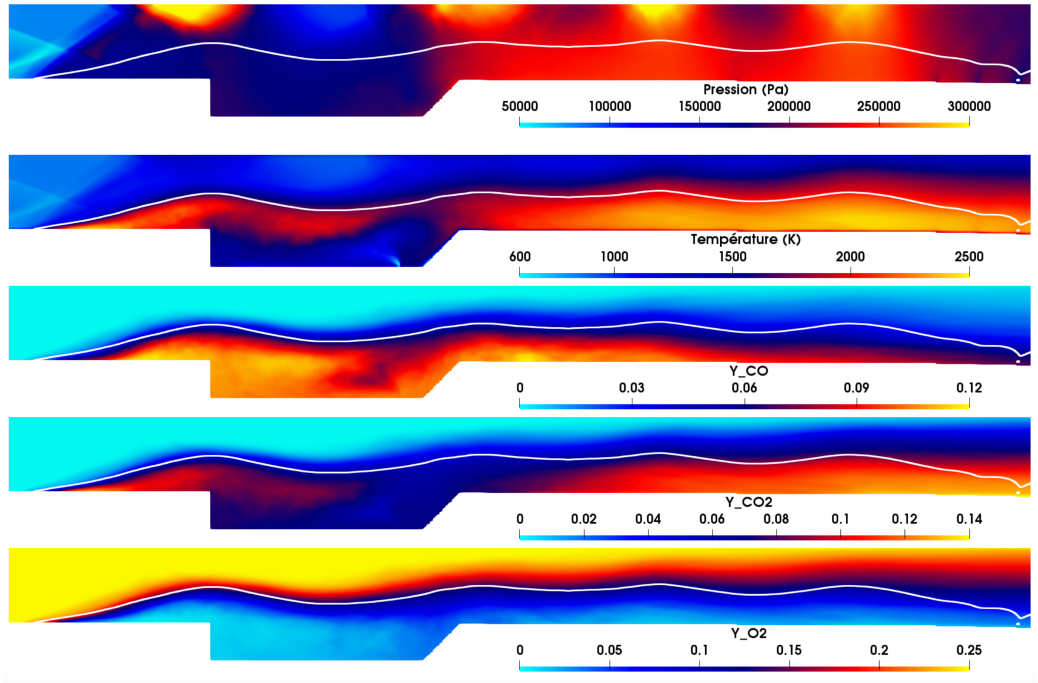

Figure 6: Mean fields of pressure, temperature and mass fractions of the major species. White line: iso-Mach $= 1$.

uniform, around 200 kPa, with a sudden increase at the boundary layer separation, marked by a compression zone and the presence of burnt gases. In the divergent, the flow presents a strong compression, linked to the expansion of the burnt gases, with a pressure plateau around 240 kPa. This blockage by the burnt gases slows down the reactive flow, thereby increasing the residence time. The mass fraction of CO shows that combustion is incomplete at the cavity, since the oxygen level is low. CO fills the cavity but its production decreases around the spray trajectory, due to the lower temperatures. CO_2 production, resulting from CO oxidation, occurs in the boundary layer separation and especially downstream of the cavity, at the thermal blockage and predominantly in the subsonic regions. Thus, the chronology from evaporation to combustion of N-decane is as follows:

- The droplet spray gradually fills the left side of the cavity, heats up, and evaporates due to a temperature above 1000 K. A small proportion of droplets interacts directly with the mixing layer;
- The evaporated kerosene mixes in the cavity, using the recirculation and pyrolysis zones, interacting in the high-temperature zones;

- A portion of the kerosene reacts at the boundary layer separation;
- The other portion reacts downstream of the cavity and to a lesser extent in the mixing layer.

The combustion process is driven by the transport of kerosene in the recirculation at the cavity, thus increasing its residence time in the combustion chamber and allowing pyrolysis and mixing with oxygen and burnt gases in the mixing layer. The oxygen present in the main flow is separated from the fuel, injected into the cavity, and the two mix and react in the mixing layer. Since combustion occurs primarily upstream and downstream of the cavity, residence time becomes a critical point in controlling the ignition, stabilization, or extinction of the flame.

4 Conclusion

LES of the CARDC supersonic cavity has been performed, starting with pilot hydrogen injection followed by a spray kerosene injection leading to a flame stabilised above the cavity. Focusing on the spray flame, the combustion process is sustained by the entrainment of kerosene droplets in the recirculations created by the cavity, thus increasing their residence time in the combustion chamber and allowing evaporation, pyrolysis and mixing with oxygen and burnt gases in the mixing layer. The oxygen present in the main flow reacts in the mixing layer with the vaporised kerosene mixed with burnt products.

References

[1] Urzay, J., "Supersonic combustion in air-breathing propulsion systems for hypersonic flight," *Annu. Rev. Fluid Mech.*, Vol. 50, 2018, pp. 593.

[2] Barnes, F. and Segal, C., "Cavity-based flameholding for chemically-reacting supersonic flows," *Prog. Aerosp. Sci.*, Vol. 76, 2015, pp. 24.

[3] Seleznev, R., Surzhikov, S., and Shang, J., "A review of the scramjet experimental data base," *Prog. Aerosp. Sci.*, Vol. 106, 2019, pp. 43.

[4] Yu, G., Li, J., Chang, X., and Chen, L., "Investigation of Kerosene Combustion Characteristics with Pilot Hydrogen in Model Supersonic Combustors," *J. Propul. Power*, Vol. 17 (6), 2001, pp. 1263.

[5] Yang, K., Pan, Y., Wang, Z., Wang, N., and Li, X., "Experimental investigation of the ignition characteristics of vaporized RP-3kerosene in supersonic flow," *Acta Astronaut.*, Vol. 174, 2020, pp. 1.

[6] Ren, X. and Wang, B., "Supersonic spray combustion subject to scramjets : Progress and challenges," *Prog. Aerosp. Sci.*, Vol. 105, 2019, pp. 40.

[7] Shen, W. and Huang, Y., "Improved delayed detached eddy simulation of supersonic combustion fueled by liquid kerosene," *Fuel*, Vol. 313, 2022.

[8] Yao, W., Wu., K., and Fan, X., "Influences of domain symmetry on supersonic combustion modeling," *J. Propul. Power*, Vol. 35 (2), 2019, pp. 451.

[9] Yu, G., Li, J., and Zhao, J., "An experimental study of kerosene combustion in a supersonic model combustor using effervescent atomization," *Proc. Combust. Inst.*, Vol. 30, 2005, pp. 2859–2866.

[10] Bouheraoua, L., Domingo, P., and Ribert, G., "Large Eddy Simulation of a supersonic lifted jet flame: Analysis of the turbulent flame base," *Combust. Flame*, Vol. 179, 2017, pp. 199–218.

[11] Ruan, J., Domingo, P., and Ribert, G., "Analysis of combustion modes in a cavity based scramjet," *Combust. Flame*, Vol. 215, 2020, pp. 238–251.

[12] Ruan, J., Bouheraoua, L., Domingo, P., and Ribert, G., "Simulation of a scramjet combustor: a priori study of thermochemistry tabulation techniques," *Flow, Turbul. Combust.*, Vol. 106, 2021, pp. 1241–1276.

[13] Ruan, L., Ribert, G., and Domingo, P., "Stabilisation and extinction mechanisms of flames in cavity flameholder scramjets," *Combust. Theory Model.*, Vol. 25 (2), 2021, pp. 193–207.

[14] Kissel, F., Ribert, G., and Domingo, P., "Large-Eddy Simulations of kerosene spray combustion in a supersonic jet flow," *Aerosp. Sci. Technol.*, 2025, pp. 110164.

[15] Yao, W., Yuan, Y., Li, X., Wang, J., Wu, K., and Fan, X., "Comparative study of elliptic and round scramjet combustors fueled by rp-3," *J. Propul. Power*, Vol. 34 (3), 2018, pp. 772.

[16] Peterson, D. M., "Simulation of a round supersonic combustor using wall-modeled large eddy simulation and partially-stirred reactor models," *Proc. Combust. Inst.*, Vol. 39, 2023, pp. 3137–3145.

[17] Nicoud, F. and Ducros, F., "Subgrid-scale stress modelling based on the square of the velocity gradient tensor," *Flow, Turbul. Combust.*, Vol. 62, No. 3, 1999, pp. 183–200.

[18] Maxey, M. and Riley, J., "Equation of motion for a small rigid sphere in a nonuniform flow," *Phys. Fluids*, Vol. 26, 1983, pp. 883–889.

[19] Henderson, C., "Drag coefficient of spheres in continuum and rarefied flows," *AIAA J.*, Vol. 14, 1976, pp. 707–708.

[20] Abramzon, B. and Sirignano, W., "Droplet vaporisation model for spray combustion calculations," *Int. J. Heat Mass Transf.*, Vol. 9, 1989, pp. 1605.

[21] Bilger, R., "Turbulent jet diffusion flame," *Prog. Energy Combust. Sci.*, Vol. 1, 1976, pp. 87–109.